Study of the Heterometallic Bond Nature in PdCu(111) Surfaces

M. Fernández-García* and J. C. Conesa

Instituto de Catálisis y Petroleoquímica, CSIC, Campus Cantoblanco, 28049 Madrid, Spain

A. Clotet and J. M. Ricart

Departament de Química, Facultat de Química, Universitat Rovira i Virgili, Pl. Imperial Tarraco, 43005-Tarragona, Spain

N. López and F. Illas

Departament de Química-Física, Facultat de Química, Universitat de Barcelona, C/Marti i Franqués 1, 08028-Barcelona, Spain

Received: June 17, 1997; In Final Form: September 17, 1997[⊗]

In this paper a theoretical study of the bonding mechanism between heteroatoms of PdCu alloys using cluster models and several ab initio methods is reported. Models of the Pd_8Cu_{92}(111) and $Pd_{40}Cu_{60}$(111) surfaces have been analyzed. For these Cu-rich alloys, we find that surface Pd centers are negatively charged. The Pd net charge increases with the Cu/Pd atomic ratio of the alloy in parallel with a decrease of the Pd 4d electronic population. The influence of the bimetallic bond on the electronic structure of core, valence, and Fermi levels is discussed, and the apparent contradiction between the net negative charge predicted for Pd and the positive binding energy shift computed and experimentally observed in these alloys for Pd core and Pd-like valence levels is interpreted.

I. Introduction

Bimetallic systems have long been of both academic and industrial interest. The study of the heterometallic bond nature, the surface composition of these binary systems, and their interaction with simple molecules (CO, NO, H_2, ...) are current topics in surface science since the earlies 1960s.[1] Nowadays, the ever-growing number of bimetallic catalysts in use by industry has enhanced the need for a good understanding of their basic structural and electronic properties, that is, of those properties which govern the alloy chemical behavior, the ultimate goal of all the above-mentioned research.[2] Among bimetallic systems, Pd−Cu has received attention due to its use in a number of catalytic reactions including CO and alkene oxidation,[3,4] CO, benzene, and toluene hydrogenation[5,6,7] and ethanol decomposition.[7] The distribution of the metals within the bimetallic phase may be a key factor in the catalytic behavior according to the specific role of each component and the nature of the reaction being studied. Likewise, copper may play a role as an active phase,[3,4] a promoter,[7] an inert diluent,[6] or simply in stabilizing Pd against sintering processes induced during activation (reduction) treatments.[3,8,9]

The Pd−Cu binary phase diagram shows the existence of ordered and substitutionally disordered fcc alloys; CuPd and Cu_3Pd ordered phases have been described, while solid solution between both elemental components can exist over the full composition range, giving rise to the mentioned substitutionally disordered fcc structures.[10] The preparation methods of catalysts, which make use of short (period of a few hours) calcination and/or reduction treatments, favor the appearance of disordered phases,[6,9] which will be the main subject of this work. These systems present to the atmosphere mainly (111)-like close packed surfaces with no significant copper segregation, something that would be expected on the basis of strain energetic effects due to the relatively large difference in atomic radii between Cu and Pd.[9,11] On alloying, photoemission[12] and XANES studies[9] reveal the profound effects of the heterometallic bond formation on the electronic structure of the Pd and Cu components. This observation applies to the majority of the Pd binary alloys including a transition or an sp metal as a second component; in these systems core and valence levels primarily related to Pd are shifted toward higher binding energies (BEs) with respect to pure Pd. The magnitude of these shifts increases with the fraction of empty states in the valence band of the second component.[1] The bonding mechanism responsible for this behavior has been theoretically investigated or inferred from spectroscopic experimental data in several Pd alloys; charge-transfer and Pd d → sp hybridation have been claimed to be the physical origin of these phenomena. However, the proposed direction of the charge-transfer and the importance of the Pd hybridation vary from one study to another, mainly because of the lack of self-consistency in some calculations and to difficulties associated in defining charge-transfer.[1]

In this work, we have analyzed the Pd−Cu bond in two representative PdCu substitutionally disordered fcc alloys by performing ab initio molecular orbital cluster model calculations using Hartree−Fock and density functional theory (DFT) frameworks. A description of the theoretical background of the method is given in section II. This includes the key features and approximations of the cluster models, the analysis methods used to extract information form the wave functions, and the distinction between initial- and final-state effects for core level binding energies. In section III, the analysis of the bimetallic

[⊗] Abstract published in *Advance ACS Abstracts,* December 1, 1997.

S1089-5647(97)01973-1 CCC: $15.00
Published on Web 01/01/1998

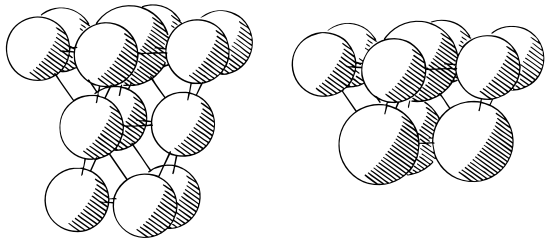

Figure 1. Schematic representation of the Pd_1Cu_{12} (left) and Pd_4Cu_6 (right) clusters used to model PdCu alloys: smaller spheres, Cu atoms; larger spheres, Pd atoms.

systems is performed by using the constrained orbital variation method (CSOV)[13−15] to decompose the interaction energy between the Pd and Cu fragments of bimetallic clusters and the Pd core level binding energy (BE) shifts into physically interpretable contributions. An orbital projection technique[16,17] will be used to obtain an estimation of the extent of the charge-transfer process between Pd and Cu on alloying. The corresponding orbital transformation (COT) of the molecular orbitals (MOs)[18] will help in analyzing Pd and Cu contributions to the valence and Fermi levels of bimetallic clusters. Correlation effects, calculated approximately by using a density functional formalism, have been computed for some of the observables. Throughout this work, particular attention will be paid to investigate the nature of the bimetallic bond and its effects on the electronic structure of the core, valence, and Fermi levels, to qualitatively interpret the experimental information already reported in the literature for Pd−Cu systems.

II. Computational Details

A. Cluster Models and Theoretical Approach. The approach used here involves choosing a small cluster to represent the surface or bulk of a compound, for which electronic wave functions are determined by ab initio or DFT quantum mechanical methods. Our primary focus is to use ab initio SCF wave functions to qualitatively study the local features of the chemical bond in Pd−Cu alloys.

To this end, we have used several clusters; below they are described and the reasons for choosing them explained. The $Pd_1(1,0,0)Cu_{12}(6,3,3)$ and $Pd_4(1,3)Cu_6(6,0)$ bimetallic clusters (Figure 1) have been taken as models of the (111) surfaces of Pd−Cu substitutionally disordered fcc alloys with, respectively, Pd_8Cu_{92} and $Pd_{40}Cu_{60}$ formal compositions. These alloys have been experimentally examined in ref 12. The Pd_nCu_m clusters (where n and m denote the number of Pd and Cu atoms, respectively) are three- (Pd_1Cu_{12}) and two-layer (Pd_4Cu_6) clusters with the number of atoms in each layer declared in parentheses. The total number of atoms in these two clusters is chosen to give a closed shell ground state within 3-fold symmetry. The first cluster intends to represent an essentially isolated surface Pd atom in a Cu matrix, while the second is chosen to represent approximately a 50/50 alloy. It must be noted that local or short-range order around Pd centers, which prefer hetero- to homoneighbors, has been recently reported;[9,19] this implies that local compositions around Pd atoms must be more Cu-rich than average ones. The chemical characteristics of the 9-fold-coordinated Pd central atom of both clusters will be the main object of this study; this atom is representative of a superficial Pd center in two different Pd−Cu environments. The PdCu disordered fcc alloys have lattice constants that correspond to a linear interpolation between the Pd and Cu bulk distances; thus atom−atom distances of 2.58 and 2.63 Å, which have been measured for the Pd_8Cu_{92} and $Pd_{40}Cu_{60}$ alloys, respectively,[12] are used in this study.

The $Pd_4(1,3)$ and $Pd_{10}(7,3)$ cluster models are also included in the calculations to serve as references for the observables calculated in bimetallic systems. The former is the Pd fragment included in the Pd_4Cu_6 system, while the latter, which has the same topology of the Pd_4Cu_6 bimetallic cluster, includes a surface Pd center equivalent to that of the bimetallic clusters. A Pd−Pd distance of 2.75 Å, corresponding to the bulk phase,[20] has been used for Pd_{10}, while the Pd_4 cluster has been calculated maintaning the distance of its parent bimetallic cluster (Pd_4Cu_6).

Results are based mainly on ab initio self-consistent-field (SCF) wave functions using the HONDO program.[21] Orbitals of ab initio SCF cluster wave functions were expanded in basis sets of contracted Gaussian functions (CGTOs). For all Pd atoms in Pd_4, Pd_{10}, Pd_4Cu_6, and Pd_1Cu_{12} clusters, relativistic effective core potentials (R-ECP) have been used to describe the 1s-3d core, while the electrons arising for the $4s^2$, $4p^6$, and $4d^{10}$ shells are treated explicitly (18-e R-ECP). The GTO's basis set for the 18-e R-ECP Pd atoms starts from the 4s, 4p, 4d, 5s, and 5p set reported in ref 22 and is contracted to [3s,3p,2d] using a nonsegmented scheme in which some GTOs are repeated to lead up to an effective 7s,5p,5d primitive set. We have checked that by using this procedure the contraction error is drastically reduced. For Cu atoms in all cases, the 1s-2p core is included in the R-ECP, while the 3s, 3p, 3d, 4s, and 4p shells are explicitly described by a GTO basis set using 7s, 5p, and 5d primitives contracted to [3s,3p,2d] using again the nonsegmented procedure described above.

Correlation effects have been taken into account for some of the observables reported by performing independent DFT calculations using the Gaussian-94 program.[23] The BLYP scheme, which includes Becke's exchange and Lee, Yang, & Parr correlation functionals (both with gradient corrections),[24] and the BPW91 one,[25] which only differs from the previous one in the use of the Perdew & Wang correlation functional, have been used here. Results are average values between both functionals, as no significative differences were observed. Same basis sets and effective core potentials have been used for both ab initio wave function and density functional based calculations.

B. Analysis of Wave Functions. To provide insights into the nature of the bonding in Pd−Cu systems, we will use several theoretical analysis methods. First, with the CSOV analysis[13−15] we decompose an observable (energy and/or core level BEs), calculated at the SCF level, into contributions arising from intraunit polarization (i.e. hybridation) and interunit charge-transfer and covalent bonding.

In the CSOV analysis, the interaction between two fragments or units A and B is analyzed by computing wave functions where variational changes from the initial separated fragments are allowed to occur in well-defined, controlled steps. Each step measures a physically interpretable contribution to the studied observable in such a way that it is decomposed in a nonbonding contribution (Pauli or steric repulsion) plus bonding contributions corresponding to internal (intrafragment) rehybridation (polarization) and interfragment charge-transfer. Step number 0 in this process corresponds to the simple superposition of the separated frozen densities (FO, frozen orbital) of both fragments; the difference between results at this stage and the simple sum of values from the fragments measures the effect of the Pauli repulsion between them. In the next step, the fragment A electron density is fixed, but the orbitals arising from fragment B are allowed to vary in their own basis space (which must be kept orthogonal to that of A), yielding the B polarization contribution to the observable. In CSOV step 2,

the A orbitals are still fixed, but now the B orbitals are varied in a space, which includes the virtual unoccupied molecular orbitals of A. This measures the effect of B to A charge-transfer, covalent bonding, and, unfortunately, the basis set superposition error (BSSE). However, the basis sets used are sufficiently large to avoid the occurrence of significative BSSE contributions.[26] In a similar way, in CSOV step 3, the A orbitals are varied in their virtual space (while B is fixed at its initial configuration), giving the A polarization contribution. Finally, in CSOV step 4, the A to B charge donation contribution is measured. The difference between the sum of all these contributions and the full SCF result yields an estimation of the completeness of the variational freedom allowed to the wave function during the CSOV procedure, so that small values of this difference evidence that essentially all important bonding effects have been taken into account during the CSOV analysis.

In our case, we define the Pd_n and Cu_m fragments (where n and m denote the number of atoms) of bimetallic clusters to be the two units A and B involved in the CSOV procedure; this allows the interpretation of intraunit polarization and interunit charge-transfer as effects of Pd on Cu or vice versa, giving physical basis to the interpretation of values obtained for the observables. The interaction energy, E_{Int}, is then defined as

$$E_{\mathrm{int}}(\mathrm{CSOV\ step}\ n) = E(\mathrm{Pd}_n) + E(\mathrm{Cu}_m) - E(\mathrm{Pd}_n\mathrm{Cu}_m;\ \mathrm{CSOV\ step}\ n) \quad (1)$$

The sign is such that a positive E_{Int} indicates a net bonding interaction. The change in E_{Int} between CSOV step n and the preceding step $n-1$, ΔE_{Int}, represents the energetic importance of the new variational freedom allowed at step n. It should be noted that the $E(Pd_nCu_m;$ CSOV step $n)$ term of (1) is not always a direct result of a simple calculation; details of its calculation can be found in refs 13−15. A similar scheme can be applied to analyze BE shifts.

The second method to characterize the bonding nature makes use of an orbital projection operator.[16,17] The projection of an orbital, $P(|\varphi\rangle)$, is the expectation value of the $|\varphi\rangle\langle\varphi|$ operator over the wave function of the system Ψ,

$$P(|\varphi\rangle) = \langle\Psi|\varphi\rangle\langle\varphi|\Psi\rangle \quad (2)$$

and measures the extent to which an orbital $|\varphi\rangle$ is contained in the total $|\Psi\rangle$ wave function. By comparing this value with that corresponding to an isolated fragment of the system, a measure of the extent of charge-transfer between Pd_n and Cu_m fragments in the Pd_nCu_m alloys can be obtained. When fractional values, between 0 and 1, are obtained, a correction for overlap of the bare Pd_n/Cu_m fragments must be performed.[17] It should be noted that this measure of the orbital charge occupation does not include any arbitrary partition of the charge density as happens with Mulliken or related charge partitioning schemes and is much less basis-dependent.[16,17] This method of charge measurement can yield a similar amount of information as charge density plots. The main problem associated with these two last methods is the partial coupling of charge polarization effects with charge-transfer processes that, in this case, are uncoupled (vide supra) by using this method in conjuntion with the CSOV tecnique presented in this section.

Finally, the analysis of the (loss of) identity of Cu and/or Pd MOs in the total wave function of the Pd_nCu_m system is made by using the so-called corresponding orbital transformation (COT).[18] For a single determinantal wave function, this is defined as the unitary transformation that leads to MOs having maximum accumulated overlap with a superposition of the Pd_n/Cu_m fragment MOs. This allows one to establish a univocal correlation between the Pd_n/Cu_m fragment MOs and the full Pd_n-Cu_m system MOs, as well as to give a measure of their changes induced by the Pd−Cu heterometallic bond formation. The overlap integrals between corresponding orbitals (COs) of a fragment and the Pd_nCu_m system are then used to do this job; a maximum similarity will get a value of 1, yielding decreasing values of the overlap integrals with increasing differences, i.e., for those MOs that are more perturbed by their participation in the interfragment bond.

C. Analysis of the Core Level BEs. Because of the important relativistic effects on the chemical behavior of Pd,[27] *all-electron* nonrelativistic Pd calculations may yield misleading results. This fact forces us to include the inner core orbitals (levels), which are experimentally measured in XPS (Pd $3d_{5/2}$),[1] in our R-ECP operator. Therefore, instead of the Pd 3d level, here we have analyzed the Pd 4s level, which has a BE of around 100 eV. It must be noted that while the 3d orbitals are core atomic like levels ($\langle r\rangle_{3d} = 0.57$ Å), the 4s is only a semicore level ($\langle r\rangle_{4s} = 0.98$ Å) having an important radial overlap with Pd valence orbitals ($\langle r\rangle_{4d} = 1.55$ Å). The importance of this difference will be discussed at length in following sections. Now, we just point out that, as will be shown later, the 3d and 4s core levels must respond (shift) in exactly the same chemical way, although simple estimations suggest that the shift magnitude can be a little lower (about 30% lower) for the 4s case.[28] To stress the necessary chemical similarity in the behavior of 3d and 4s BE values upon alloying, some *all-electron* test calculations were performed in the Pd_1Cu_{12} cluster using an extended 18s13p7d1f basis set for the Pd atom[29] while the same ECP and basis set were maintained for Cu.

It is usual to classify contributions to the BE as initial- and final-state effects (IS and FS, respectively).[26] Initial-state values are those determined solely by the electronic structure of the neutral, un-ionized system and are given by the Koopman's theorem (KT),

$$\mathrm{BE(KT)} = -\epsilon_{\mathrm{i}} \quad (3)$$

where ϵ_{i} is the SCF orbital energy of the ionized orbital. We will analyze these initial-state effects for the 4s orbital of the surface Pd center of bimetallic clusters by using the CSOV technique in a way similar to that described above for the interaction energy.

To obtain final-state BE effects, it is necessary to obtain a SCF wave function for the final n - 1 electron ionic state, $\Psi_{\mathrm{SCF}}^{(n-1)}$, where the electrons respond and are relaxed in the presence of the ionic hole. The energy of $\Psi_{\mathrm{SCF}}^{(n-1)}$ is lower that the energy of the Koopman's ionic wave function, $a_i^{\dagger}\Psi_{\mathrm{SCF}}^{(n)}$ (where $a_i^{\dagger}$ is the annihilation operator of the ith electron), by the relaxation energy E_{R}. The relaxed final-state BE is given by the SCF energy difference, ΔSCF, of the initial and final states,

$$\mathrm{BE}(\Delta\mathrm{SCF}) = E(\Psi_{\mathrm{SCF}}^{(n-1)}) - E(\Psi_{\mathrm{SCF}}^{(n)}) \quad (4)$$

and thus

$$E_{\mathrm{R}} = \mathrm{BE(KT)} - \mathrm{BE}(\Delta\mathrm{SCF}) > 0 \quad (5)$$

In general, E_{R} is quite large, from a few to hundreds of electronvolts, depending on the BE of the core level.[26] Experimental BE values correspond normally to situations where electrons have been able to relax partially during the photoionization event so that, even if the relaxation effect is lower that

TABLE 1: Interaction Energy (with Respect to the Corresponding Pd_{10} and Cu_{13} Reference Clusters), E_{Int}, and Work Function, ϕ, (eV) of Mono- and Bimetallic Clusters. Experimental Values of the Work Function, ϕ_{Exptal} (eV), for the (111) fcc Surface of Pure Metals Are Also Included for Comparison

model	E_{int}	ϕ_{SCF}	ϕ_{DFT}	ϕ_{exptal}[a]
Cu_{13}		4.08		4.94
Pd_1Cu_{12}	1.67	3.93	3.51	
Pd_4Cu_6	2.15	5.66	3.65	
Pd_{10}		7.08	4.28	5.60
Pd_{23}		6.50		5.60

[a] From ref 30.

the amount of (5), it is still essential to include final-state effects in order to obtain reasonable values for core level BEs. However, here we will concentrate on the BE change or shift occurring in the bimetallic systems with respect to the monometallic Pd reference. In many metallic systems this chemical shift is dominated by initial-state effects, allowing an interpretation in terms of the initial-state chemistry of the core-ionized atom.[26] This is also the physical reason the 3d and 4s levels (and any other core level) shift approximately by a similar amount. We must recall that initial-state core level shifts are a measure of the electric field at the nucleus. The correlation contribution to the core level BEs has been estimated using DFT calculations.

III. Results and Discussion

The energies of interaction between fragments, measured relative to those of the corresponding monometallic reference clusters, and the predicted work function (WF) values (computed with both SCF and DFT) for the cluster models considered are given in Table 1. Both values of relative E_{Int} are positive, indicating that the Pd−Cu bond is stronger that the Pd−Pd and Cu−Cu bonds, in agreement with the known ability of alloying between both metals. The experimental WFs of the (111) surfaces of the pure metals are also included in this table for comparison purposes.[30] The computed WF in Pd-containing systems increases regularly with the Pd percentage in the alloy composition, suggesting a smooth transition in the valence band (VB) characteristics from Pd to Cu. This overall increasing behavior, observed for both DFT and ab initio SCF calculations, qualitatively matches the experimental difference between values for the pure metals, although the magnitudes of the WFs calculated are far from the experimental ones due to the known limitations of the cluster approach in predicting WF values. These limitations come from the incomplete representation of the alloy VB.[31] Note, however, that the cluster calculations, which contain the local features of the intermetallic bond, do correctly mimic the WF behavior along the Pd−Cu series, as this is driven by the predominance of Cu-like subbands in Cu-rich alloy Fermi regions and of Pd-like ones in Pd-rich specimens.

To analyze the bonding mechanism between Pd and Cu in Pd−Cu alloys, the CSOV decomposition of the interfragment interaction energy is given in Table 2. Before commenting on it, let us point out that, from one cluster to other, the atom−atom distance varies and the units/fragments defined to make the CSOV (Pd_n and Cu_m) have different numbers of atoms. Both factors hinder an easy interpretation of the nonbonding FO step values presented in Table 2. The Pd_n polarization and the Pd_n and Cu_n donations are the principal, bonding contributions to the interaction energy. Among polarization (i.e. hybridation change) contributions, the Pd_n one is always larger than that

TABLE 2: CSOV Analysis for the Interaction Energy ($E_{Int}/\Delta E_{Int}$; eV) between Pd_n and Cu_m Fragments of Bimetallic Clusters. the (Pd_4Pd_6) Calculation Is Included as a Reference (See Text for Details)

CSOV step	Pd_1Cu_{12}	Pd_4Cu_6	(Pd_4Pd_6)
0. FO	−1.51/...	−0.45/...	−1.32/...
1. Pol. Cu_m	−1.09/0.42	−0.16/0.29	.../0.17
2. Don. Cu_m	−0.14/0.95	1.61/1.77	.../0.61
3. Pol. Pd_n	0.56/0.70	2.75/1.14	.../0.19
4. Don. Pd_n	1.50/0.94	3.84/1.09	.../0.60
5. SCF	1.76/0.29	4.14/0.30	.../0.03

taking place in Cu. As the main contribution to energy changes in the Pd/Cu polarization process comes from the d → sp internal hybridation, this difference in magnitude is likely to arise from the fact that only high-lying Cu sp band orbitals can be used as empty states for Cu polarization due to the significant electronic occupation of this subband, while for the Pd fragment, the much smaller occupation of the corresponding outermost sp band and the lower energetic difference between occupied d states and empty sp ones would allow a larger polarization contribution. The Pd_n donation energy term is nearly the same in both bimetallic systems studied, while the Cu_n donation term grows with the percentage of Cu in the alloy composition. The physical origin of these contributions will be later analyzed by complementing this analysis with the projection operator technique to measure the electron charge-transfer associated with these two steps.

The significance of heteroatomic effects in the values obtained for Pd_4Cu_6 has been roughly ascertained with the CSOV procedure by comparing with the Pd_4Pd_6 (Pd_{10}) cluster. Note that, although the atom−atom distances in these two clusters are different, they correspond to a linear compensation of the difference in metallic radii between Pd and Cu, so that, to a first approximation, the comparison allows the extraction of the differential chemical response of Pd to two environments. Thus, from this calculation we can see that the presence of Cu (instead of Pd) intensifies the Pd_n polarization contribution, while the Pd_n donation in much less affected. As the FO repulsion is larger in the Pd_4Pd_6 reference system, the enhancement of the Pd polarization by the presence of Cu should probably be ascribed to preparation for covalent bonding. The lower effect in the Pd_n donation step will be interpreted below on the basis of the charge-transfer study. The SCF step completes the CSOV analysis; the small contribution in this final step (≈0.3 eV, less than 15% of the interaction energy) comes from coupling among the different orbital variation steps allowed to occur individually during the CSOV procedure.

To estimate the nature and extent of the charge-transfer processes occurring upon alloy formation, the (accumulated) projections of the five 4d and one 5sp orbitals (per atom) of the surface Pd center and of the Pd_n fragment and those of the five 3d and one 4sp orbitals (per atom) of the Cu_m fragment on the total (system) wave function have been used to compute the occupation values of these levels. Results are given in Table 3. Notice that for the surface Pd center the overlap correction is done only in the Pd_1Cu_{12} cluster; for Pd_4Cu_6, the methodology allows this to be done easily only for the Pd_4 fragment as a whole, but such correction is found to be very small, and therefore data for the Pd^S atom (given without that correction) can be taken as accurate enough.

The first point to remark on these projection results is that the starting Pd_n fragments ($n = 1, 4$) used to build the bimetallic clusters have a surface Pd center with an electronic configuration close to $d^{10}s^0$. However, for Pd_{10} this Pd atom has opened significantly its 4d shell by hybridation with the 5sp orbitals.

TABLE 3: Expectation Values (Electrons/Increment of Electrons) of the 4d and 5sp Orbitals in the Central Surface Pd Atom (Pd^S) and Pd_n Fragment (Pd^F) for Mono- and Bimetallic Clusters, and of the 3d and 4sp Orbitals of the Cu_n Fragment (Cu^F) for Bimetallic Clusters

orbital	Pd_1	Pd_1Cu_{12}	Pd_4	Pd_4Cu_6	Pd_{10}
Pd^S(4d)	10.00/0.00	9.75/−0.25	9.98/−0.02	9.84/−0.16	9.89/−0.11
Pd^S(5sp)	0.00/0.00	0.60/+0.60	0.02/+0.02	0.27/+0.27	0.11/+0.11
Pd^F(4d)				39.79/−0.21	
Cu^F(3d)		120.00/0.00		60.00/0.00	
Cu^F(4sp)		11.65/−0.35		5.52/−0.48	

TABLE 4: Overlap Integrals, λ, between COs for Some Orbitals of Pd_n/Cu_m Fragments and the Pd_nCu_m Systems.[a] λ Values Are Presented in Increasing Order of Energy of the COs (i.e. Values Corresponding to Deeper Levels Are Given First)

orbitals	clusters	λ(symmetry)[b]
Pd^S(4d)	Pd_1Cu_{12}	0.990(A_1); 0.995(E); **0.972(E)**
	Pd_4Cu_6	0.990(A_1); 0.993(E); **0.972(E)**
Cu^F(4sp)	Pd_1Cu_{12}	0.997(A_1); **0.977(A_1)**[c]; 0.993(E)[c]; **0.939(E)**[c]
	Pd_4Cu_6	**0.928(A_1)**[c]; **0.980(E)**[c]

[a] Cu^F(3d) orbitals give $\lambda > 0.999$. [b] λ values smaller than 0.99 are boldfaced. [c] Values corresponding to orbitals lying above the Pd^S(4d) ones. Last value corresponds to the cluster HOMO.

This electronic rearrangement in going from small clusters (Pd_4 or smaller) to larger ones (Pd_{10}) has been previously reported for cluster models of the Pd(100) surface.[27] In Pd_4Cu_6, the opening of the 4d shell in the surface atom approaches that observed in the Pd cluster with the same total number of atoms, Pd_{10}, although is somewhat larger (0.16 vs 0.11 electrons). For Pd_1Cu_{12}, this 4d shell is even less occupied. In both cases, the (chemical) effect of changing Pd by Cu at the neighbor positions on the occupation of these 4d orbitals of the central Pd is only of moderate magnitude. On the other hand, the projection study shows the null role of the 3d Cu subband in the alloy formation; the Cu (chemical) contribution to the bimetallic bond is performed through the 4sp subband. Most apparent in both bimetallic systems is the net Cu_m to Pd_n charge-transfer (measured through the Cu 4sp depopulation), particularly for the Pd_4Cu_6 one, giving physical support to the more important energy variation observed for this cluster during the CSOV procedure in the Cu to Pd donation step. The magnitude of the global Cu_m to Pd_n charge-transfer process depends obviously on the balance between the number of acceptor and donor atoms; our data suggest that its maximum amplitude is reached when both kinds of atoms are present in nearly equal amounts. Note, however, that the effect on some observables as Pd BEs depends more on the amount of charge-transferred per Pd atom, which is larger in Pd_1Cu_{12}.

The CSOV and projection analyses thus evidence the complex mechanism of alloying. The heterometallic bond formation induces loss of charge in the Pd 4d and Cu 4sp subbands and a net gain in the Pd 5sp one, all charge-transfer processes growing with the Cu content of the alloy (Table 3). The major electronic rearrangement occurs within the sp subband. The Cu 3d orbitals do not contribute to the bond, and the Pd 4d suffers only moderate loss of charge; for alloy compositions near 50/50, the 4d charge deficiency at the central Pd atom is comparable to that of pure Pd metal. The results of the CO study, presented in Table 4, concur in this analysis, showing the larger extension of the orbital mixing in the sp subbands, which lose their single metal characteristics in becoming the highest part of the bimetallic VB. The Pd 4d subband maintains its single metal properties in the alloy to a substantial extent. Such a notable effect in the alloy sp subband has been observed experimentally by XANES, being particularly evident in the Cu K-edge 1s → 4p transition (where 4p is a pd hybrid state with primarily p character) corresponding to the 9000 eV continuum resonance.[9] XPS and photoemission studies[12,32] show the existence of pronounced Pd-like features below the Fermi level for copper-rich samples. The conclusions reached there about the bonding mechanism, similar in both papers, differ in some details from the conclusions in this work; in fact some of these studies suggest a possible Cu 3d contribution to the bond[32] and, in general, do not consider the role of the Pd 5sp orbitals.[12,32] These papers do, however, concur with this study in pointing out the important electronic rearrangement induced by the intermetallic bond, the existence of strong Pd-like features in the VB, and the Cu-like character of the Fermi region. Briefly, the analysis of the binary Pd−Cu bond provides evidence of the metallic (covalent) nature of the interaction but also detects a small charge-transfer contribution which negatively charges Pd; the excess charge is located in the outermost sp band. The only previous study of charge-transfer effects in Pd−Cu systems was reported by Rocherfort and Fournier for the bimetallic dimer; after a Mulliken population analysis, they suggest, contrarily to this study, the existence of a net Pd to Cu charge transfer.[33] Without considering the possible artifacts derived from the Mulliken analysis, the difference can be explained on the basis of the extremely short Pd−Cu distance in the dimer, i.e., 2.32 Å (about 0.34 Å shorter than the one corresponding to a $Pd_{50}Cu_{50}$ alloy). This should exalt the Pd 4d participation in the bond and, consequently, the Pd(4d) → Cu(4sp) charge-transfer contribution with respect to extended Pd−Cu alloys.

The interpretation of the heterometallic bond just outlined allows one to understand several experimental observations. We first concentrate in the Fermi region. Analysis of COs (Table 4) denotes the Cu 4sp dominant role in the Fermi region for Cu-rich alloys, in agreement with experimental reports,[12,32] although the overlap integrals of several Cu 4sp-based COs and the electron population figures (Table 3) give evidence of the nonnegligible Pd 5sp contribution to these higest lying levels. This fact may help to rationalize the, up to now not clearly understood, energetic behavior of probe molecules (CO, NO, ...) during adsorption on Pd−Cu alloys.[1,33−35] The CO adsorption energetics is a balance between bonding (CO σ donation and π back-donation) and antibonding (i.e. Pauli repulsion) contributions. The substrate, in the case of Pd or Cu, uses mainly the d orbitals for the more important bonding contribution (π back-donation) and involves the sp levels (levels in or close to the Fermi level) in the steric repulsion with the adsorbate.[27,34] As the main differences among Pd−Cu alloys occur in the outermost sp region, it may be predicted that the larger local sp occupation of Pd centers will reduce the energy of CO adsorption over these centers by the increase of the Pauli repulsion, and conversely, the loss of sp charge in Cu centers of Pd−Cu alloys will increase the Cu−CO interaction energy; such changes have been experimentally observed.[32,35] Note, however, that the d subband metal contribution has been claimed to be predominant in determining the CO/metal interaction energy.[36] It is expected that a CSOV analysis may help to clarify this issue; such a study is now in progress and will be reported separately.[37]

Another characteristic property of the Pd alloys is the displacement to higher BEs suffered by the Pd-like features of the VB. This Pd 4d-like feature of the VB becomes stabilized in Pd−Cu alloys, moving down away from the Fermi energy, by the reduction of the electron−electron repulsion within that

TABLE 5: CSOV Analysis of the 4s Semicore Level BE (eV) for the Surface Pd Atom of Bimetallic Clusters. Total (Initial and Initial+Final) Shifts and Relaxation Energy (eV) Are Given with Respect to the Surface Pd Atom of the Pd_{10} Cluster. A (Pd_4Pd_6) Reference Calculation Is Also Included (See Text for Details)

contribution	Pd_1Cu_{12}	Pd_4Cu_6	(Pd_4Pd_6)
1. Pol. Cu_m	−0.55	−1.15	−0.44
2. Don. Cu_m	−0.54	−0.74	−0.30
3. Pol. Pd_n	3.31	2.67	1.09
4. Don. Pd_n	1.41	0.79	0.16
5. SCF	−0.28	−0.23	−0.01
$TOTAL^I$	2.40 [1.36][a]	1.11 [0.78][a]	
E_R	0.30	0.32	
$TOTAL^{I+F}$	2.10	0.79	

[a] Values between brackets correspond to DFT calculations including correlation corrections.

TABLE 6: SCF Orbital Energies (eV) for the 3d and 4s Core Levels of Atomic Pd and the Pd_1Cu_{12} Cluster (from *All-Electron* Calculations) and Shift (eV) Calculated between These Systems for Both Levels

system	3d	4s
atomic Pd	−362.20	−96.49
Pd_1Cu_{12}	−382.72/−382.85	−117.42
shift (Pd_1Cu_{12} - Pd)	−20.65	−20.93

electron shell induced by a postulated loss of charge that, in turn, is believed to exist due to Pd to Cu charge transfer and/or Pd rehybridation.[1,38] Our analysis however shows that the decrease in occupancy calculated here for the 4d orbitals of a surface Pd atom in the alloy, expressed relative to the monometallic Pd reference, is minimal, close to zero for a 50/50 alloy composition. Because the analysis of the heterometallic bond formed shows that the major electronic rearrangement related to alloying occurs in the outermost sp subband region, we suggest that these changes must be the physical origin of the specific energetic behavior (i.e. of the electrostatic potential variations) of the alloy VB. Similar arguments based on electronic rearrangements mainly due to charge polarization effects have been claimed to account for the lowering of Pd-like VB features in several bimetallic interfaces.[39] On the other hand, the difficulties in the accurate representation of the VB inherent to the cluster model approach do not allow us to discuss in more detail the alloy VB.

To complete the study of the influence of the heterometallic bond formation in the electronic properties of a Pd surface center in Pd−Cu alloys, in Table 5 the CSOV decomposition of the initial-state 4s semicore level BE is presented. To show that changes in BE values of this level parallel those of the (usually measured in XPS experiments) 3d levels, these BEs have been computed in *all-electron* calculations (as described in section 2.C) for the isolated Pd atom and for the Pd_1Cu_{12} cluster. The results are given in Table 6, which confirms that the 4s-based analysis of the XPS shifts can be totally equivalent to a 3d-based one. Both levels shift (as expected) in the same direction and to a similar extent; just a small 0.3 eV difference is observed over a total shift of about 21 eV. So, the better adequacy of the 4s level (which includes relativistic effects in a simple way) for theoretical studies does not have any detrimental effect on the extraction of the chemical consequences of the intermetallic bond formation with respect to 3d-based XPS data.

First to note from Table 5 is that the 4s level BE shift is dominated by initial-state effects ($E_R \approx 0.3$ eV, i.e., 25% of the initial-state contribution), allowing an interpretation of the BE shift in terms of changes in the initial energy levels due to differences in the chemical environment sensed by the surface Pd center. A core eigenvalue initial-state shift can be described as the sum of the electronic changes occurring when going from one environment to the other. The most common situation is the dominance of the Coulomb part, so that changes in core eigenvalues are a direct measure of changes in the electrostatic potential value measured near the nucleus (the core levels region) of the atom.[28] The change or shift in BEs thus comes from changes in the $\langle 1/r \rangle$ expectation value for the core−electron orbital to be ionized. Consequently, processes that move charge away from inner regions of the atom will produce positive shifts, while negative ones are induced by charge moving closer to the nucleus. This allows the interpretation of the signs obtained in the CSOV decomposition; while Cu_m polarization and donation move charge close to the central Pd atom to prepare and perform (respectively) covalent bonding between fragments, Pd donation to Cu moves charge away from this central Pd atom, and Pd polarization moves electronic charge from 4d levels to 5sp ones, i.e., also away from the nucleus and core levels. The donation and polarization contributions of the Pd_n fragment and those of Cu_m tend to cancel each other due to their different sign. Although the four contributions have significant magnitude, that due to Pd_n polarization is, at least, 2 times larger than the others. As mentioned above, a much larger polarization contribution of Pd can be expected on the basis of the local emptiness/occupancy of the outermost sp subband. Additionally, the electrostatic potential variations induced by electronic rearrangements of Pd must be larger than Cu ones due to the closeness to the (Pd) nucleus of the 4d charge density involved. On the other hand, the comparison of the Pd polarization contribution magnitude of both bimetallic clusters and the (Pd_4Pd_6) reference suggests that the enhancement of this contribution with respect to Pd metal is proportional (Table 5) to the number of heteroneighbors in the first coordination shell. The final result is that initial-state contribution to the shifts calculated (at the SCF level) is of considerable magnitude. Correlation effects (see bracketed values in Table 5) make a nonnegligible correction, which becomes more significant in the Pd_1Cu_{12} cluster, but clearly do not invalidate the trends here reported.

In Pd alloys, the magnitude of Pd core level shifts in both surface and bulk Pd atoms has been shown to increase with the fraction of empty states in the VB of the second component of the binary alloys.[1,38] Two mechanisms have been claimed to account for this behavior: polarization (hybridation) within the Pd atom and charge transfer between the alloy components. The quantification of the importance of these two phenomena is rather difficult to obtain from experimental measurements and, up to now, has not been done theoretically. For Pd−Cu alloys the results in Table 5 show that, for a surface Pd atom, the Pd polarization is the leading term and that net charge-transfer process (Pd donation + Cu donation) makes only a moderate to low contribution to the total shift, around 0.87 eV (or 33% of the initial-state contribution) for Pd_1Cu_{12} and 0.05 eV (4%) for Pd_4Cu_6. Important to stress again is that the net shift is a result of incomplete cancellation between Pd and Cu physical contributions of opposite sign due to the complex nature of the heterometallic bond which includes charge-transfer processes in both directions (Pd to Cu and Cu to Pd), so that the shift is dominated by an important Pd polarization contribution. Consequently, no direct relation should be drawn between net charge on Pd and Pd core level shifts, at least for Pd−Cu alloys.

The $TOTAL^{I+F}$ shift with respect to the vacuum level amounts to ≈2.1 and 0.8 eV for the Pd_8Cu_{92} and $Pd_{40}Cu_{60}$ alloys, respectively, and ≈1.4 and 0.5 eV with respect to their Fermi level (estimating the Fermi energy by linear interpolation

between the experimental pure metal measurements). Correlation effects may reduce these figures by 1.0 and 0.3 eV, respectively, giving an estimation of the 4s semicore level shift of ≈1.1 and 0.5 eV with respect to the vacuum level and ≈0.4 and 0.2 eV with respect to the Fermi level. The increasing positive shift with alloy Cu content is in agreement with experimental results available only for the $3d_{5/2}$ level (≈0.75 and 0.45 eV for Pd_8Cu_{92} and $Pd_{40}Cu_{60}$ alloys, respectively),[1,12,38] although the computed magnitude for the Pd_8Cu_{92} alloy may be a little bit excessive. Note that, as mentioned in section II, the shallow 4s core level may shift a little less than the $3d_{5/2}$ core level due to the smaller Columbic interaction of the former level with the valence shell. It should be also noted, on the other hand, that the Pd line asymmetry introduces some uncertainty in the BE shifts experimentally measured.[12] To conclude with the analysis of the core levels, it can be mentioned that, as already suggested,[12] the Cu predominance in the Fermi region of Cu-rich alloys introduces a significant change with respect to Pd-rich alloys in the local density of states near the Fermi level, which will change the shape asymmetry of the XPS peaks, as experimentally observed.[1,12,38]

V. Conclusions

We have reported theoretical results of the nature and characteristics of the heterometallic bond in the (111) surface of PdCu alloys using several cluster models and ab initio SCF wave and DFT density functions. Our focus was the study of the alloying effects on a surface Pd center. The neighboring presence of Cu produces an internal Pd d → sp rehybridation (Pd polarization) larger than that corresponding to pure metallic Pd. This can be explained on the basis of the stronger character of the hetero- vs homometallic bond; the introduction of Cu in the solid induces a higher extent of Pd polarization as a prerequisite for bonding, which occurs mainly via sp levels. Additionally, a Cu(4sp) → Pd(5sp) charge-transfer process is detected which leaves the surface Pd atom negatively charged. Minor electron density transfer from the Pd 4d shell to Cu is observed, while the Cu 3d shell does not participate in the heterometallic bond.

Despite the net negative charge detected in surface Pd centers, the Pd 4s semicore level is predicted to shift to higher BEs, as experimentally found for other Pd core levels in these alloys. The reason is that the 4s BE shift is dominated by the extent of the 4d Pd depopulation, and this is determined mainly by the initial-state Pd polarization, which is highly sensitive to the chemical nature of the core-ionized atom environment (its contribution is proportional to the number of Cu neighbors located around a Pd center). This conclusion can be generalized to any other Pd core level provided that it is initial-state driven. It has been thus shown that the sign and magnitude of the BE shift is not a valid parameter to measure the extent of charge transfer between alloy components of PdCu systems.

Acknowledgment. M. F.-G. thanks the Consejo Superior the Investigaciones Científicas (CSIC) for a Postdoctoral Contract under which this work has been carried out. Financial support by CICyT (Projects MAT94-0835-CO3-02 and PB95-0847-CO2-01) and CAM (Project 06M/085/96) is fully acknowledged. The authors wish to thank the Centre de Supercomputació de Catalunya (CESCA) for helping in part of the calculations.

References and Notes

(1) Rodriguez, J. A. *Surf. Sci. Rep.* **1996**, *24*, 223.
(2) Ponec, V.; Bond, G. C. *Catalysis by Metals and Alloys*; Elsevier: Amsterdam, 1995.
(3) Choi, K. I.; Vannice, M. A. *J. Catal.* **1991**, *131*, 36.
(4) Espeel, P. H.; De Peuter, G.; Trelen, M. C.; Jacobs, P. A. *J. Chem. Phys.* **1994**, *98*, 11588.
(5) Anderson, J. A.; Fernández-García, M.; Haller, G. L. *J. Catal.* **1996**, *164*, 477.
(6) Leon y Leon, C. A.; Vannice, M. A. *Appl. Catal.* **1191**, *69*, 305.
(7) Skoda, F.; Astier, M. P.; Pajonk, G. M.; Primet, M. *Catal. Lett.* **1994**, *29*, 159.
(8) Fernández-García, M.; Márquez-Alvarez, C.; Haller, G. L. *J. Phys. Chem.* **1995**, *99*, 12565.
(9) Fernández-García, M.; Anderson, J. A.; Haller, G. L. *J. Phys. Chem.* **1996**, *100*, 16247.
(10) Villards, A. P.; Calvet, L. D. *Pearson's Hanbook of Crystallographic Data for Intermetallic Phases*; ASM Int.: OH, 1991.
(11) Vurens, G. H.; Van Delft, F. C. M. J. M.; Niewenhuys, B. E. *Surf. Sci.* **1987**, *192*, 428.
(12) Martensson, N.; Nyholm, R.; Calén, H.; Hedman, J.; Johansson, B. *Phys. Rev. B* **1981**, *24*, 1725.
(13) Bagus, P. S.; Herman, K.; Bauschlicher, C. W. *J. Chem. Phys.* **1984**, *80*, 4378.
(14) Bagus, P. S.; Herman, K.; Bauschlicher, C. W. *J. Chem. Phys.* **1984**, *81*, 1966.
(15) Bagus, P. S.; Illas, F. *J. Chem. Phys.* **1992**, *96*, 8962.
(16) Pacchioni, G.; Illas, F.; Philpott, M. P.; Bagus, P. S. *J. Chem. Phys.* **1989**, *90*, 4287.
(17) Bagus, P. S.; Illas, F. *Phys. Rev. B* **1990**, *42*, 10852.
(18) Amos, A. T.; Hall, G. C. *Proc. R. Soc. (London)* **1961**, *A263*, 483.
(19) Murray, P. W.; Stensgaard, I.; Laegsgaard, E.; Besenbacher, F. *Surf. Sci.* **1996**, *365*, 591.
(20) Wyckoff, R. W. G. *Crystal Structures*, 2nd ed; Wiley: New York, 1963; p 10.
(21) Dupuis, M.; Johston, F.; Márquez, A. *HONDO 8.5 for CHEMstation*; IBM Corporation: Neighborhood Road, Kingston, NY 12401, 1995. CSOV adaptation by Illas, F.; Rubio, J.; Márquez, A.
(22) Hay, P. J.; Wadt, W. R. *J. Chem. Phys.* **1985**, *82*, 299.
(23) Frisch, M. J.; Trucks, G. W.; Schlegel, H. B.; Gill, P. M. W.; Johnson, B. G.; Robb, M. A.; Cheeseman, J. R.; Keith, T.; Petersson, G. A.; Montgomery, J. A.; Raghavachari, K.; Al-Laham, M. A.; Zakrzewski, V. G.; Ortiz, J. V.; Foresman, J. B.; Peng, C. Y.; Ayala, P. Y.; Chen, W.; Wong, M. W.; Andres, J. L.; Replogle, E. S.; Gomperts, R.; Martin, R. L.; Fox, D. J.; Binkley, J. S.; Defrees, D. J.; Baker, J.; Stewart, J. P.; Head-Gordon, M.; Gonzalez, C.; Pople J. A. *Gaussian 94, Revision B.3*; Gaussian, Inc.: Pittsburgh, PA, 1995.
(24) Becke A. *Phys. Rev. A* **1988**, *38*, 3098; Lee, C.; Yang, W.; Parr, R. G. *Phys. Rev. B* **1988**, *37*, 785.
(25) Perdew, J. P.; Wang, Y. *Phys. Rev. B* **1992**, *45*, 13244.
(26) Bagus, P. S.; Brundle, C. R.; Pacchioni, G.; Parmigiani, F. *Surf. Sci. Rep.* **1993**, *19*, 265.
(27) Pacchioni, G.; Bagus, P. S. *J. Chem. Phys.* **1990**, *93*, 1209.
(28) Egelhoff, W. F. *Surf. Sci. Rep.* **1987**, *6*, 253.
(29) Waite, J. Private communication.
(30) *CRC hanbook of Chemistry and Physics*, 72nd ed.; CRC: Boca Raton, 1992.
(31) Pettersson, L. G. M.; Bagus, P. S. *Phys. Rev. Lett.* **1986**, *56*, 500.
(32) Rochefort, A.; Abon, M.; Delichère, P.; Bertolini, J. C. *Surf. Sci.* **1993**, *294*, 43.
(33) Rochefort, A.; Fournier, R. *J. Phys. Chem.* **1996**, *100*, 13506.
(34) Herman, K.; Bagus, P. S.; Nelin, C. J. *Phys. Rev. B* **1987**, *35*, 9467.
(35) Debauge, Y.; Abon, M.; Bertolini, J. C.; Massardier, J.; Rochefort, A. *Surf. Sci.* **1995**, *90*, 15.
(36) Hammer, B.; Morikawa, Y.; Norskov, J. K. *Phys. Rev. Lett.* **1996**, *76*, 2141.
(37) Fernández-García, M.; Conesa, J. C.; Clotet, A.; Ricart, J. M.; López, N.; Illas, F. To be published.
(38) Rodriguez, J. A. *Surf. Sci.* **1994**, *318*, 253.
(39) Wu, R.; Freeman, A. J. *Phys. Rev. B* **1995**, *52*, 12419.